THE JOURNAL OF PHYSICAL CHEMISTRY C

Article

pubs.acs.org/JPCC

Copper Coordination Study in a Metal-Induced Chiral Polythiophene Aggregate

Juan Torras*,† and Carlos Alemán‡,§

†Department of Chemical Engineering, Igualada School of Engineering, Universitat Politècnica de Catalunya, Pça Rei 15, Igualada 08700, Spain

‡Department of Chemical Engineering, Barcelona School of Industrial Engineering, Universitat Politècnica de Catalunya, Diagonal 647, Barcelona E-08028, Spain

§Centre for Research in Nano-Engineering, Universitat Politècnica de Catalunya, Campus Sud, Edifici C′, C/Pasqual i Vila s/n, Barcelona E-08028, Spain

ABSTRACT: The chiral regioregular polythiophene, poly[(*R*)-3-(4-(4-ethyl-2-oxazolin-2-yl)phenyl)-thiophene] (PEOPT), forms chiral aggregates in chloroform under copper salt presence, with chirality disappearing upon the addition of acetonitrile. We report here a comprehensive quantum mechanical study of intermolecular assembly adducts with a copper ion that may be involved in this switching process. Results indicate that copper adducts made of undissociated copper salt in chloroform prefer a *syn*-$(EOPT)_2$ disposition of ligands belonging to different polythiophene chains, favoring a double-stranded helical conformation. In contrast, doped polymer with copper ions in acetonitrile prefers an *anti*-$(EOPT)_2$ arrangement for the different polythiophene side chains, favoring a nonchiral π-stacked packing. Furthermore, another cross-linked interaction besides the most stable NN-type has been characterized. Thus, NO-type interactions on the $[Cu(EDOT)_2]Cl_2$ adducts in chloroform have been shown to be energetically stable. However, hybrid quantum mechanical/molecular mechanical molecular dynamics (QM/MM MD) simulations indicate that only those adducts that involve helical chains keep structural stability under kinetic considerations.

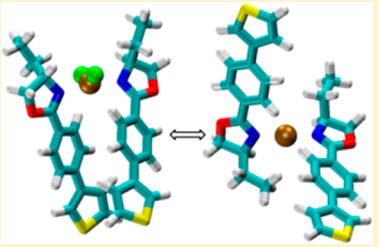

INTRODUCTION

Supramolecular chemistry has been extensively studied due to its importance in a wide variety of polymeric systems where capabilities such as assembly, conformation, and/or behavior are extended beyond the molecule (e.g., protein[1] and polymers[2]). Usually, highly directional noncovalent interactions such as hydrogen bonding, metal coordination, and $\pi-\pi$ interactions are responsible to hold a stable supramolecular structure. Among them, whether or not metal is present allows quickly switching some chemical and physical properties of supramolecular compounds that make them useful as chemisensors.[3] Also, modern coordination chemistry enables us to mimic many of the biological shapes, improving the potentiality of new supramolecular structures in polymer chemistry.[4,5]

On the other hand, polythiophene derivatives (PTs) are among the most interesting and useful π-conjugated polymers due to their interesting electronic and optical properties.[6−8] Concretely, chiral PTs have attracted particular interest due to their chiroptical properties[9−11] and potential applications (e.g., circular polarized electroluminescence devices and enantioselective sensors).[12,13] Recently, an interesting capability to induce supramolecular chirality in achiral PTs via chiral information transfer from chiral PT chains has been reported.[14] Also, there is the possibility to switch aggregation by means of regulating on the solvent medium.[15,16] Goto et al.[12,15] found that a chiral, regioregular (head-to-tail) PT, poly[(*R*)-3-(4-(4-ethyl-2-oxazolin-2-yl)phenyl)-thiophene] (hereafter PEOPT, Scheme 1) containing an optically active oxazoline residue in the side group, forms self-assembled supramolecular chiral aggregates with intermolecular π-stacking interactions by the addition of poor solvents to a chloroform solution. However, Yashima et al.[13] previously reported that PEOPT chirality also could be induced through complexation with metal ions in good solvents, such as chloroform. Those authors point out that the oxazoline residue capability to form metal coordination interactions between different chains is responsible for building helical arrangements with a well-defined handedness. More specifically, nitrogen atoms from two oxazoline moieties which

Scheme 1

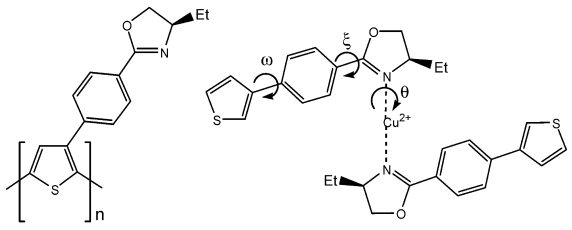

PEOPT $[Cu(EOPT)_2]^{2+}$

Received: January 31, 2014
Revised: April 13, 2014
Published: April 16, 2014

   dx.doi.org/10.1021/jp501118y | *J. Phys. Chem. C* 2014, 118, 9769−9779

belong to two different non-π-stacked polymer chains were coordinated with a metal ion such as Cu^{2+}, Cu^{+}, and Fe^{3+}, the two last ions being involved in a relatively weak complex formation in chloroform (Scheme 1). More recently it has been shown that chiral information transfer from PEOPT can also be applied to an achiral PT with an oxazoline group in the side chain using a good solvent. Goto et al.[17] proposed that this new chirality might be obtained through specific metal ions which are used as intermolecular cross-linking agents via metal coordination to the oxazoline residues between both polymer types.

However, the most exciting ability of PEOPT aggregates in terms of supramolecular chirality is the reversibility (on−off) of the aggregation phenomenon by the addition or removal of an electron from the polymer main chain. Specifically, an alternate addition of Cu^{2+} and a copper complexing agent leads to reversible changes on the induced circular dichroism (ICD) of polymer aggregates.[18]

Comprehensive theoretical studies about the structural molecular properties of PEOPT have been shown by two stable molecular arrangements on short oligomers. The first consists of a plain structure which allows the formation of a π-stacking alignment between phenyl groups of adjacent monomers, while the second is a helical structure with six repeating units per turn.[19] Moreover, a recent theoretical study of models of PEOPT aggregates shows two different possible structures of aggregates depending on oligomer length: a self-assembled helical aggregate was found for short oligomers, whereas a bent double-helix aggregate was obtained for large oligomers.[20]

Emergence of chiral polythiophenes is getting more relevance in the field of supramolecular chemistry due to their specific electrical and optical properties, although these are still poorly understood. Computational analysis may give insights and predict properties and potential uses of these chemical systems. The metal-induced aggregation, and more specifically the PEOPT aggregation by metal coordination, has been studied but still remains a challenge from both theoretical and experimental points of view. The aim of the present paper is to study by means of quantum mechanics (QM) and hybrid quantum mechanical/molecular mechanical molecular dynamics (QM/MM MD) methodologies the coordination structure of a cooper ion (Cu^{2+}) with short and large PEOPT oligomers in different solvents. Accordingly, the paper is organized as follows. Initially, a QM study is performed to characterize the coordination structures and stability of complexes made of a Cu^{2+} ion with one and two EOPT monomer units, considering different solvent polarities. To evaluate the role played by counterions in the adduct formation, which is not clear, counteranions such as Cl^{-} have been considered. Finally, two chains complexed through a Cu^{2+} ion have been modeled using a hybrid QM/MM MD calculation. Both helical (*syn−gauche*, hereafter *all-sg*) and elongated (*anti−gauche*, hereafter *all-ag*) structures have been considered in QM/MM MD simulations to investigate the influence of the metal coordination in secondary structure of the polymer.

METHODS

Quantum Mechanical Calculations. Density functional theory (DFT) calculations have been carried out using the Gaussian 09 computer program,[21] by combining the Becke's three-parameter hybrid functional (B3)[22] with the Lee, Yang, and Parr (LYP)[23] expression for the nonlocal correlation (B3LYP). All DFT calculations in this work have been performed by combining the B3LYP method with a mixed basis set (hereafter MBS) made of 6-31+G(d)[24] and an effective core potential LANL2DZ (Los Alamos National Laboratory 2 Double-Zeta)[25] basis set. The latter was used on the transition metal, whereas the Pople-type basis set is used on all other atoms. LANL2DZ is a widely and well-tested ab initio effective core potential (ECP) to model metal atoms in combination with Pople-type basis sets.[26]

Geometry optimizations were performed without any restriction in the gas phase and in implicit solvent. Free energies were estimated by frequency calculations to obtain the zero-point vibrational energies and both the thermal and entropic corrections. Binding energies (BEs) were calculated for the $[Cu(EOPT)_2]Cl_2$ only and corrected with the basis set superposition error (BSSE) by means of the standard counterpoise (CP) method but incorporating relaxation energy into correction.[27] The binding energy of adducts is defined as usual by

$$BE^{CP} = E_{adduct} - [2E_{EOPT} + E_{CuCl2}] + E_{BSSE}$$

where E_{adduct} is the ab initio DFT energy of the optimized adduct, whereas E_{EOPT} and E_{CuCl2} are the ab initio DFT energies of the optimized isolated EOPT ligand unit and $CuCl_2$, respectively. The proposed BE definition will allow us to study energy interactions and adduct stability between nondissociated copper salt and EOPT units.

Besides gas-phase calculations, we also optimized the solvated structures of $[Cu(EOPT)_n]^{2+}$ and $[Cu(EOPT)_2]Cl_2$ adducts in chloroform and acetonitrile starting from previously derived geometries on the gas phase. The polarizable continuum model (PCM)[28,29] was used for the bulk solvent effect. All PCM calculations were calculated at the B3LYP/6-31+G(d) LANL2DZ level and considering the dielectric constants of chloroform (ε = 4.71) and acetonitrile (ε = 35.69). The relative free energies (ΔG_r) and the binding energies in solution, which provide information about the relative stability of the complexes and the strength of the interactions in solution, respectively, were computed using the same scheme as in the gas phase.

Hybrid QM/MM MD Calculations. QM methodology allows characterizing the geometries of complexes involving the metal coordination with one or two EOPT monomeric units but has no explicit account of solvent molecules, kinetic energy, and stiffness of polymer backbone structure. The influence of this factor was evaluated by applying a multiscale approach based on an explicit solvation model of chloroform to investigate the metal coordination stability on two different secondary structures of the polymer chain: helical and extended. In this method, the atomic motions are handled by molecular dynamics (MD), energies and forces being calculated by dividing the system into two different parts. The metal-coordinated complex is treated at the quantum mechanical (QM) level, while molecular mechanics (MM) are applied to the rest of the system (polymer and solvent) by using a classical potential energy function.

In this work, two basic secondary structures were considered for the polymer, namely, the helicoidal (*all-sg*) and extended (*all-ag*) conformations, exhibiting an inter-ring dihedral angle between adjacent thiophene moieties ($\theta_{S-C-C-S}$) of 36.1° and 120°, respectively. Each one of these structures contains two chains with 15 repeating units (15-EOPT) arranged according to a head-to-tail (H−T) disposition, which were linked through

dx.doi.org/10.1021/jp501118y | J. Phys. Chem. C 2014, 118, 9769−9779

two oxazoline moieties (one from each chain) coordinated to one Cu^{2+} ion and neutralized with two chloride ions. Finally, the systems were solvated with 4138 chloroform molecules, thus defining a minimum of 10 Å buffer region around each complex. Solvent molecules were described using the Cieplak et al.[30] model. All force field parameters for the solute molecules were extrapolated from the generalized AMBER force field (GAFF)[31] with the exception of the torsional barrier associated with the inter-ring dihedral angle S−C−C−S between consecutive thiophene rings, which was derived from a previous work.[32] All trajectories were carried out using the AMBER12[33] software package.

Previous to the production the QM/MM MD trajectory, the two constructed systems were minimized at the MM level, heated to 298 K, and finally equilibrated using an NPT ensemble for 0.1 ns (1 fs time steps). In both thermalization and equilibrations steps the atomic positions of solute were restrained to the initial geometry by a force constant of 5 kcal/mol·Å^2. Thus, the weak coupling method of the Berendsen thermo-barostat[34] was used to control the temperature and pressure of the system by means of a time constant for the heat bath coupling and a pressure relaxation time of 8 and 2 ps, respectively. In all cases, atom pair distance cutoffs were applied at 15 Å to compute van der Waals interactions. Electrostatic interactions were computed using the nontruncated electrostatic potential by means of Ewald summations.

Hybrid QM/MM MD calculations were run using the PUPIL interface,[35,36] which allows us to link, among others, QM calculations from the NWChem[37] program with MD simulations from the AMBER12[33] program. The starting structures using the NWChem−PUPIL−Amber interface[38] on the QM/M MD simulation were extracted from the last classical MD equilibration snapshot. Subsequently, two repeating units (EOPT) without the thiophene moiety, one from each chain, and the linking $CuCl_2$ molecule were changed to a QM description, while the chloroform molecules remained within the MM framework. Thus, all atoms except copper from the QM region were described by combining the B3LYP functional with the 6-31G basis set, whereas the metal atom was modeled by the effective core potential LANL2DZ basis set. After that, the systems were allowed to relax for 10 ps (0.5 fs time step) without any restriction and using a constant-pressure simulation with the same parameters previously used for fully classical MD simulations. Periodic boundary conditions were applied in the preparation of the NWChem input to wrap neighboring point charges around the quantum region. The coordinates of relaxing trajectories on the last 6 ps were saved for subsequent analysis, discarding the first 8000 steps of the hybrid QM/MM MD simulation.

RESULTS AND DISCUSSION

Quantum Mechanics Structural Study. This section presents the structural study of the complex formed between the Cu^{2+} ion and EOPT monomer, results obtained in the gas phase being compared with those obtained in an implicit solvent model of increasing polarity (i.e., chloroform and acetonitrile). This study was performed using a three-step strategy. First, the stability of complexes formed by a Cu^{2+} ion coordinated with a single EODT was determined, allowing us to locate the more favored interaction sites. For this purpose, interactions between the metal ion and different EOPT moieties with an excess of electronic charge were considered. Specifically, the following five interacting sites were used to construct the initial complexes: the N and O atoms of oxazoline, the phenyl and thiophene aromatic rings, and the S atom of the thiophene moiety. After this, once identified the relative stability of the different sites of metal−ligand interaction, a new adduct made of a Cu^{2+} ion, and two monomeric units of EOPT was considered. The latter complex simulates the cross-linking between two monomeric units belonging to different chains due to metal coordination, as noted by previous experimental data.[13,39] Finally, the stability of neutral complexes was studied by introducing new ions, such as Cl^-, which might induce some steric and electronic changes in the new $[CuEOPT_2]Cl_2$ complex, which in turn may change the stability order of those characterized minima.

[CuEOPT]$^{2+}$. Table 1 lists the structural parameters together with the relative energy (ΔE_r) and relative free energy (ΔG_r) of the minimum energy structures characterized in the gas phase, chloroform and acetonitrile for the $[CuEOPT]^{2+}$ adducts, where the Cu^{2+} ion is interacting with different EOPT moieties. The nomenclature X−Cu used to denote the new adducts refers to the main ligand−metal interaction considered. Also, Figure 1 shows the minimum energy structures characterized in the gas phase. The most stable adduct is the N−Cu, in which the copper ion is directly faced toward the oxazoline ring, located at a distance of 1.934 Å from the N atom. Furthermore, the metal ion is also close to one of the hydrogen atoms belonging to the terminal methyl group of EOPT (d_{Cu-H} = 2.002 Å). Thus, the proximity of the methyl moiety leads to an increase of the agostic interactions between the terminal methyl group and the copper center, as indicated by the slight

Table 1. Structural Properties of Selected Minimum Energy Structures of $[CuEOPT]^{2+}$ Adducts Calculated at the B3LYP/6-31+G(d) LANL2DZ Level in the Gas Phase and Different Solvents[c]

system	d_{Cu-X}[a]	θ'[b]	ξ	ω	ΔE_r	ΔG_r
			Gas Phase			
EOPT	-		0.6	43.3	-	-
N−Cu	1.934	8.3	23.1	3.4	0.0	0.0
S−Cu	3.010	163.8	−0.2	−29.0	20.4	19.7
S−Cu′	2.286	−164.5	−0.6	−29.3	22.8	22.0
O−Cu	1.968	141.8	−22.8	−5.3	27.2	26.3
Ph−Cu	2.154	136.1	3.6	5.5	31.7	31.0
			Chloroform			
N−Cu	1.931	6.5	31.4	−3.1	0.0	0.0
S−Cu	3.147	168.0	−1.9	15.5	17.0	15.5
S−Cu′	2.296	−163.0	−0.1	−20.2	20.6	18.8
O−Cu	2.011	148.9	−27.5	−6.4	20.3	19.6
Ph−Cu	2.192	133.8	1.7	1.8	21.9	20.4
			Acetonitrile			
N−Cu	1.932	6.3	32.1	−0.6	0.0	0.0
S−Cu	3.213	165.7	−0.3	12.4	15.0	14.8
S−Cu′	2.310	−168.1	0.1	4.7	19.2	18.2
O−Cu	2.026	147.6	−27.3	0.2	17.8	17.9
Ph−Cu	2.192	132.9	1.1	−0.5	18.1	17.1

[a]Bond distance between copper and coordinated ligand. X refers to the atom from the ligand bonded to metal: N (N−Cu), O (O−Cu), S (S−Cu), and C (Ph−Cu). [b]Dihedral angle between the oxazoline moiety plane and the copper ion (N−C−O−Cu). [c]Dihedral angles (θ', ξ, and ω; see Scheme 1) in degrees; bond distance (d_{Cu-X}, d_{N-C}, and d_{N-C}) in Å; relative energy (ΔE_r) and relative free energy (ΔG_r) in kcal/mol.

dx.doi.org/10.1021/jp501118y | J. Phys. Chem. C 2014, 118, 9769−9779

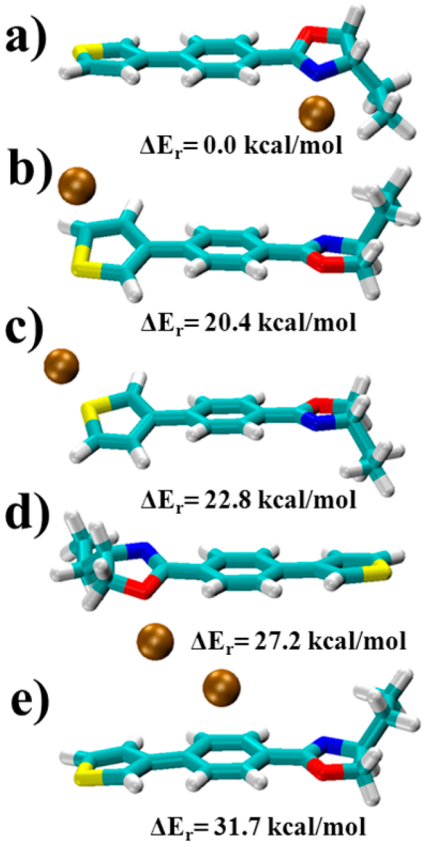

Figure 1. Minimum energy conformations obtained for $[CuEOPT]^{2+}$ adducts in the gas phase: (a) N−Cu, (b) S−Cu, (c) S−Cu′, (d) O−Cu, and (e) Ph−Cu.

elongation observed in the strong C−H and C−C bonds when compared with those in the isolated EOPT (i.e., d_{C-H} = 1.119 Å and d_{C-C} = 1.534 Å for the adduct; d_{C-H} = 1.098 Å and d_{C-C} = 1.512 Å for uncomplexes EOPT). The N−Cu adduct induces charge transfer between the metal ion and the EOPT monomeric unit, which leads to a light p-type doping of EOPT. In fact, charge population analysis based on the atomic polar tensor (APT) charge[40] reflects a positive charge accumulation on the thiophene group (not shown) that is consistent with the coplanarity between the thiophene and benzene rings (ω = 3.4°) .

The second and third adducts with the lowest relative free energy are those with the copper ion located close to the thiophene ring. Specifically, S−Cu and S−Cu′ adducts are 19.7 and 22.0 kcal/mol, respectively, less stable than the absolute minimum. In these cases the positive charge is accumulated on the benzene and oxazoline rings with an almost planar dihedral angle, ξ. The most unstable adducts are O−Cu and Phe−Cu. Interestingly, APT charges (not shown) indicate a polarization of the EOPT unit with the positive charge mainly located at the thiophene ring and distributed between thiophene and benzene rings for S−Cu and S−Cu′, respectively. The oxazoline ring presents in both cases a lightly negative charge of ∼0.2 au.

Increasing the polarity of the environment makes the ΔG_r gap of adducts shrink, while the stability order established in the gas phase is preserved. Thus, the relative free energy difference between the second and the last adduct from the series is 11.3, 4.9, and 2.3 kcal/mol in the gas phase, chloroform, and acetonitrile, respectively. Regarding changes on the adduct geometries, the variation of the polarity does not provoke significant distortions on the bond distances and dihedrals angles. Interestingly, there is a tendency to elongate a little bit the bond distance between the copper ion and the EOPT unit (d_{Cu-X}) as the polarity increases, even though this distance is kept almost constant in the Cu−N adduct.

$[Cu(EOPT)_2]^{2+}$. Table 2 lists the structural parameters together with the relative free energy (ΔG_r) for the minimum energy conformations characterized in the gas phase, chloroform, and acetonitrile of the $[Cu(EOPT)_2]^{2+}$ adducts. Similarly to previous adducts, the interaction of the Cu^{2+} ion with several EOPT moieties has been considered. However, each metal−ligand interaction has been modeled using two different orientations regarding the EOPT units, *syn*-$(EOPT)_2$ and *anti*-$(EOPT)_2$ conformations. Concretely, taking into account the longitudinal axis of the EOPT unit (from oxazoline up to the thiophene moiety), the arrangement obtained when both EOPT axes are laid out in parallel pointing to the same direction (<90°) is named *syn*-$(EOPT)_2$. However, when both axes are laid in opposite directions (>90°), the resulting disposition is named *anti*-$(EOPT)_2$. In the nomenclature of new adducts, XY, both letters X and Y are referring to the main metal−ligand interaction considered at each one of the two EOPT units (e.g., NO refers to an adduct involving N−Cu and

Table 2. Structural Properties of Selected Minimum Energy Conformations of $[CuEOPT_2]^{2+}$ Adducts Calculated at the B3LYP/6-31+G(d) LANL2DZ Level in the Gas Phase and Different Solvents[b]

system	d_{Cu-X}[a]	θ	ξ	ω	ΔG_r
			Gas Phase		
NN	1.922	124.4	−19.1	16.4	0.0
			−19.6	15.4	
NN′	1.928	−124.9	22.6	16.9	0.7
			20.3	15.9	
NN″	1.923	−39.6	−22.3	−15.3	3.4
			−21.9	−14.9	
NO	1.910	−122.9	−21.7	18.1	21.0
	1.970		−18.8	−14.5	
			Chloroform		
NN	1.919	126.9	−24.8	13.4	0.0
			−25.0	12.5	
NN′	1.917	−7.4	−26.7	−11.4	0.0
NO	1.912	−163.6	19.4	2.8	18.3
	1.988		29.2	25.1	
NO′	1.912	−152.8	18.9	1.8	18.7
	1.993		31.9	26.2	
			Acetonitrile		
NN	1.922	124.7	−25.0	27.3	0.0
			−28.3	2.4	
NN′	1.920	−7.9	−26.7	−25.5	0.4
			−25.4	3.0	
NN″	1.927	−129.7	30.7	−2.3	2.1
			27.0	26.7	
NO	1.916	−154.4	20.5	0.5	16.5
	1.990		28.4	25.7	
NO′	1.915	152.7	−24.5	−0.2	17.7
	1.993		−27.5	25.2	

[a]Bond distance between copper and coordinated ligand. X refers to the atom from the ligand bonded to metal. [b]Dihedral angles (θ, ξ, and ω; see Scheme 1) in degrees; bond distance (d_{Cu-X}) in Å; relative free energy (ΔG) in kcal/mol.

dx.doi.org/10.1021/jp501118y | J. Phys. Chem. C 2014, 118, 9769−9779

O−Cu interactions from the first and second EOPT units, respectively). Figure 2 shows the minimum energy conformations characterized in the gas phase.

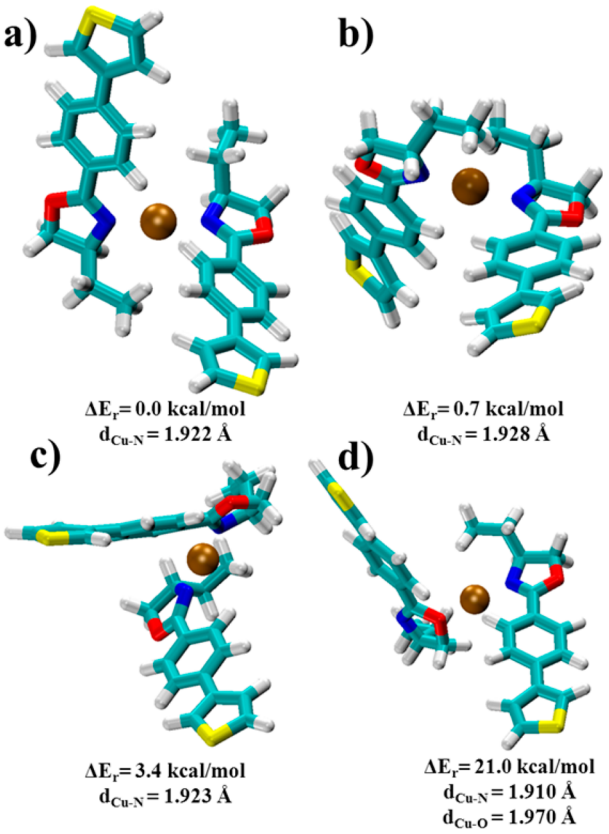

Figure 2. Minimum energy conformations obtained for $[CuEOPT_2]^{2+}$ adducts in the gas phase: (a) NN, (b) NN′, (c) NN″, and (d) NO.

The most stable adduct in the gas phase is the NN, which presents an *anti*-$(EOPT)_2$ disposition between both EOPT ligands (θ = 124.4°), the distance between the metal ion and the N atoms located at different EOPT units being 1.922 Å. Interestingly, this minimum does not present as clear agostic interactions with the closest hydrogen atom of each EOPT unit, which represents a difference with respect to the absolute energy minimum of $[CuEOPT]^{2+}$. However, the final optimized geometry (Figure 2a) has the copper ion in a pseudocage made of two hydrogen atoms that belong to different benzene rings (2.606 and 2.631 Å) and two hydrogen atoms from different ethyl moieties (2.658 and 3.008 Å).

The second most stable adduct in the gas phase (NN′), which also involves the copper ion coordinated with two nitrogen atoms, is destabilized by 0.7 kcal/mol with respect to the lowest energy one. The NN′ adduct has an *anti*-$(EOPT)_2$ arrangement between both EOPT ligands, with a dihedral angle θ = −124.9°. The Cu−N bond distance (1.928 Å) is slightly larger than that of the absolute energy minimum, but the positive charge is hindered in a pseudocage with shorter Cu−H distances with the neighbors' hydrogen atoms. Concretely, besides the N ligands, the closest atoms to the copper ion are the hydrogen atoms from the benzene rings (2.444 and 2.442 Å) and those from the ethyl moieties (2.541 and 2.509 Å). The third adduct is 3.4 kcal/mol unfavored and also presents a coordination with two nitrogen atoms (NN″) but with a *syn*-$(EOPT)_2$ disposition between both EOPT ligands (θ = −39.6°). In that case the charge screening by closer hydrogen atoms is not as clear as previous NN adducts. However, it can be appreciated that there is a slight increment in the dihedral angle ξ with increasing instability of NN adducts, which is mainly related by the p-doping effect by induced charge polarity as seen above in the $[CuEOPT]^{2+}$ adducts. Finally, the last adduct shown is the NO, which is destabilized by 21 kcal/mol with respect to the absolute minimum of energy in the gas phase (NN adduct). This adduct presents an *anti*-$(EOPT)_2$ disposition. Also, there is a clear difference in the dihedral angles between ring moieties, ξ and ω, in both sides of the EOPT unit ligand.

Furthermore, other adducts such as OO, SS, and PhePhe have been also found in the gas phase (not shown), even though with relative free energy higher than 37 kcal/mol. Due to these large destabilizations, they have not been considered to be studied with implicit solvent. The increase of environment polarity does not alter the absolute minimum of energy, the *anti*-$(EOPT)_2$ being the most stable disposition. However, the *syn*-$(EOPT)_2$ arrangement (NN′) is almost isoenergetic, with 0.0 and 0.4 kcal/mol of relative free energy in chloroform and acetonitrile, respectively. The stability of the highest energy NO′ adduct increases with the polarity, the relative free energies being 21.0, 18.7, and 17.7 kcal/mol in the gas phase, chloroform, and acetronitrile, respectively. This behavior is similar to that observed for monoligand adducts, $[CuEOPT]^{2+}$.

$[Cu(EOPT)_2]Cl_2$. Similarly to previous subsections, a study involving neutral adducts at different solvent polarity has been carried out. Thus, a nondissociated salt effect that might happen on weakly polar solvents has been considered. Table 3 lists the structural parameters together with the ΔG_r and the binding energy (BE) values for the minimum energy structures characterized in the gas phase, chloroform, and acetonitrile for neutral $[Cu(EOPT)_2]Cl_2$ adducts. Figures 3, 4, and 5 show the minimum energy structures of those neutral adducts obtained in the gas phase, chloroform, and acetonitrile, respectively. For all three environments only stable adducts with negative BE values are presented.

The incorporation of chloride ions to build adducts without net charge leads to a predominance of *syn*-$(EOPT)_2$ arrangements (Table 3), which represents a difference with respect to what was observed for ionic adducts (i.e., *anti*-$(EOPT)_2$ arrangements were the most stable is for $[CuEOPT_2]^{2+}$; Table 2). In this scenario, the most stable adduct in the gas phase is the NN, which presents a *syn*-$(EOPT)_2$ disposition (θ = −0.3°) and a Cu−N bond distance of 2.042 Å (Figure 3a). The inclusion of Cl^- ions as additional ligands, besides the steric perturbation between EOPT units, also leads to a weaker Cu−N interaction that is reflected by the increment of the Cu−N bond distance (∼0.12 Å). In spite of this, the absolute minimum remains very stable with a BE of −18.2 kcal/mol. In addition, the *syn*-$(EOPT)_2$ arrangement allows a displaced-parallel π-stacking interaction between the two benzene rings and the two thiophene rings of different EOPT units, with a distance between their respective centers of mass of 4.83 and 5.36 Å, respectively. Moreover, a significant decrease in the induced charge polarity of EOPT is observed. This is highlighted by the ω dihedral angle, which shows a significant increase with respect to those of previous $[Cu(EOPT)_2]^{2+}$ adducts (Table 2).

The next adduct (NN′), which is destabilized by 3.3 kcal/mol, presents a *syn*-$(EOPT)_2$ conformation with a displaced-parallel π-stacking interaction between both benzene rings

dx.doi.org/10.1021/jp501118y | J. Phys. Chem. C 2014, 118, 9769−9779

Table 3. Structural Properties of Selected Minimum Energy Conformations of $[Cu(EOPT)_2]Cl_2$ Adducts Calculated at the B3LYP/6-31+G(d) LANL2DZ Level in the Gas Phase and Different Solvents[b]

system	d_{Cu-X}[a]	d_{Cu-Cl}	α_{ClCuCl}	θ	ξ	ω	ΔG_r	BE
				Gas Phase				
NN	2.042	2.336	161.9	−0.3	−24.3	31.4	0.0	−18.2
NN′	2.066	2.339	160.5	−4.6	−25.0	−28.3	3.3	−15.1
NN″	2.053	2.308	148.5	−104.9	−24.3	31.0	10.1	−7.1
	2.109	2.315			22.3	32.1		
NO	2.028	2.278	151.5	−71.9	−28.9	29.0	10.9	−5.9
	2.219	2.271			20.0	31.5		
NO′	2.044	2.281	171.6	−124.3	−23.0	−31.8	12.5	−4.5
	2.207				−22.2	30.2		
				Chloroform				
NN	2.033	2.363	154.6	−8.6	−25.7	26.4	0.0	−17.9
NN′	2.046	2.368	160.0	−8.1	−25.3	−27.0	5.3	−13.8
						−26.5		
NN″	2.082	2.340	143.2	−85.5	−26.1	27.0	8.4	−9.5
	2.052	2.338			−22.0	28.5		
NO	2.016	2.294	152.1	−68.6	−30.1	26.3	11.7	−5.5
	2.200	2.301			22.8	29.8		
NO′	2.025	2.306	172.3	−130.4	−25.7	−30.0	13.0	−3.6
	2.210	2.292			−28.0	28.0		
				Acetonitrile				
NN	2.030	2.375	154.2	−8.8	−26.4	25.5	0.0	−17.5
NO	1.962	2.228	145.9	−44.9	29.4	26.9	7.4	−6.0
	4.800	2.232			3.1	28.1		
NO′	2.014	2.305	156.5	−63.6	23.8	29.2	11.9	−5.0
	2.191	2.312			−29.9	24.9		
NO″	2.022	2.300	172.0	−130.8	−26.7	−28.5	13.8	−3.2
	2.209	2.314				26.8		

[a]Bond distance between copper and the coordinated ligand. X refers to the atom from the EOPT ligand bonded to metal. [b]Bond angle (α_{ClCuCl}) and dihedral angles (θ, ξ, and ω; see Scheme 1) in degrees; bond distances (d_{Cu-X} and d_{Cu-Cl}) in Å; relative free energy (ΔG_r) and binding energy (BE) in kcal/mol.

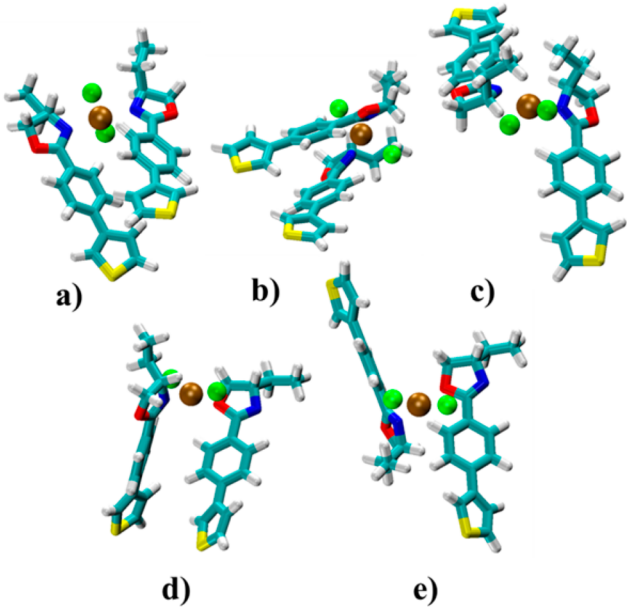

Figure 3. Minimum energy conformations obtained for $[Cu(EOPT)_2]Cl_2$ adducts in the gas phase: (a) NN, (b) NN′, (c) NN″, (d) NO, and (e) NO′.

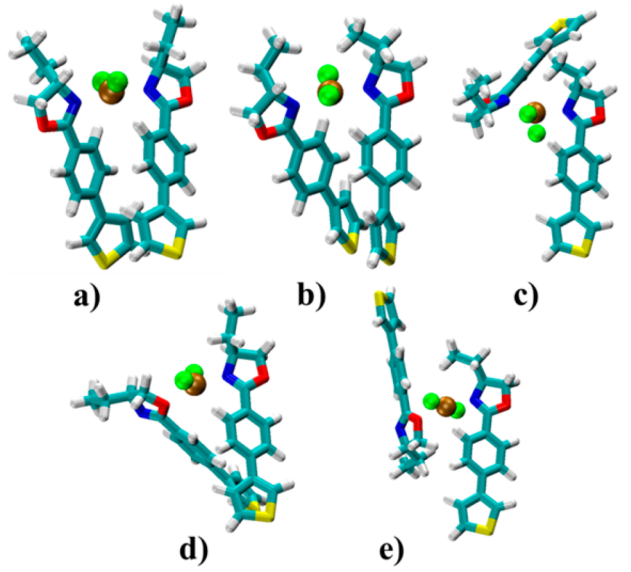

Figure 4. Minimum energy conformations obtained for $[Cu(EOPT)_2]Cl_2$ adducts in chloroform: (a) NN, (b) NN′, (c) NN″, (d) NO, and (e) NO′.

separated by a distance of 4.45 Å. The Cu−N interaction is slightly weaker than in the absolute minimum with a similar steric disposition but with crossing over EOPT units. The third NN″ adduct is higher in relative free energy but still holds a stable BE of −7.1 kcal/mol. This structure reflects unsymmetrical Cu−N interactions, forcing an *anti*-$(EOPT)_2$ disposition. Thus, EOPT units show a perpendicular-like arrangement

dx.doi.org/10.1021/jp501118y | J. Phys. Chem. C 2014, 118, 9769−9779

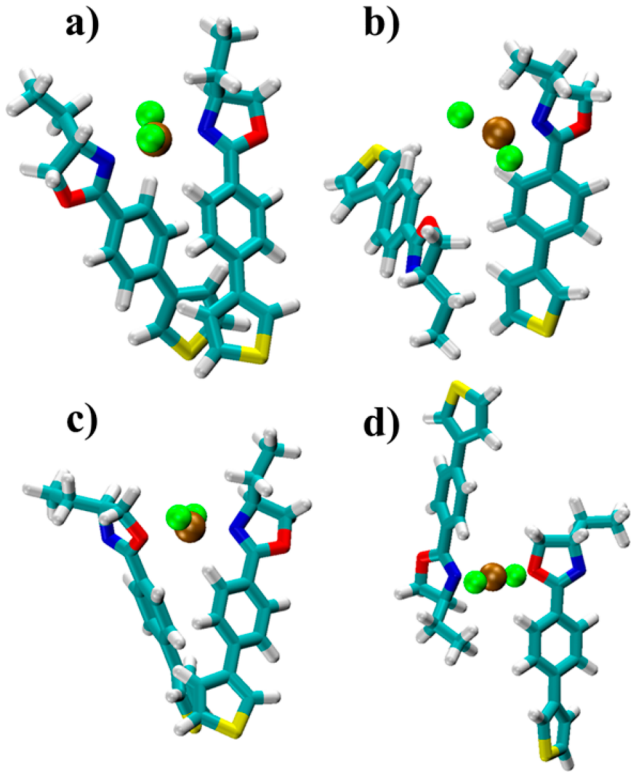

Figure 5. Minimum energy conformations obtained for [Cu-(EOPT)$_2$]Cl$_2$ adducts in acetonitrile: (a) NN, (b) NO, (c) NO′, and (d) NO″.

that is clearly unfavorable when compared with previous *syn*-(EOPT)$_2$ of NN-type adducts.

On the other hand, the only stable adducts involving different oxazoline moiety atoms are the NO and NO′ with BEs of −5.9 and −4.5 kcal/mol, respectively (Figures 3d and 3e). The former holds a *syn*-(EOPT)$_2$ conformation with a crossing over of EOPT units that stabilize a T-shaped stacking between benzene rings with a distance of 5.03 Å between their centers of masses. The latter adduct, NO′, presents the most clear *anti*-(EOPT)$_2$ conformation (θ = −124.3°). Although his structure does not allow a π-stacking between EOPT units, it keeps similar Cu−X bond distances and dihedral angles to the NO adduct.

Minimum energy structures displayed in Figure 4, which correspond to those characterized in chloroform, are similar to those obtained in the gas phase with a predominance of *syn*-(EOPT)$_2$ conformations. Specifically, the NN adduct, which is the absolute minimum with a BE of −17.9 kcal/mol, holds a benzene···benzene π-stacking with a distance between centers of masses (4.44 Å) shorter than the stacking distance found for the NN aduct in the gas phase (4.83 Å).

Moreover, the BE of stable NO and NO′ adducts is −5.5 and −3.6 kcal/mol, respectively, the latter being the only one with an *anti*-(EOPT)$_2$ disposition. Thus, the ΔG_r and the BE increase slightly when adducts change from the gas phase to chloroform solution.

Figure 5 shows the four [Cu(EOPT)$_2$]Cl$_2$ stable adducts characterized in acetonitrile. Interestingly, in this solvent only one stable NN-type adduct (NN), with *syn*-(EOPT)$_2$ geometry, π-stacking distances (d_{ThTh} = 5.42 Å and d_{PhPh} = 4.45 Å), and BE (−17.5 kcal/mol) similar to the absolute minimum in chloroform, was obtained. Furthermore, three different NO-type adducts were found. As occurred in the gas-phase and chloroform solution, the highest energetic but stable NO″ adduct (BE = −3.2 kcal/mol) is the only one with an *anti*-(EOPT)$_2$ disposition. Solvent polarity enhancement induces small variations in the bond lengths, the Cu−N and Cu−O bonds becoming slightly more weak and strong, respectively, than in chloroform solution. Interestingly, the NO adduct (BE = −6.0 kcal/mol) is an unbalanced adduct with one of the EOPT ligands favoring Cu−N interaction in detriment of the Cu−O one (i.e., Cu−X distances of 1.962 and 4.800 Å with X = N and O, respectively).

Hybrid QM/MM MD Structural Study. Experimental evidence showed that CuCl$_2$ induces supramolecular chirality of the PEOPT aggregates in chloroform. Usually, metal salts used to form adducts with PEOPT are insoluble in this good solvent. Also, the low polarity of chloroform leads to an expected undissociated salt molecule in this environment. Moreover, counteranions have been found to affect significantly the adduct formation, even though the reasons for their influence are not clear yet.[39] In this work theoretical calculations predict that the presence of chloride counteranions favors the *syn*-(EOPT)$_2$ disposition compared with the favored *anti*-(EOPT)$_2$ conformation of the ionic adducts such as [CuEOPT$_2$]$^{2+}$.

This kind of metal-induced chiral aggregation has been previously studied experimentally, and in addition, some theoretical models of NN-type adducts involving aggregate structures made of all-*sg* and all-*ag* conformations of PEOPT were proposed.[39] However, the counteranion effect examined in this work at the QM level also shows a stable interaction involving NO-type adducts with an *anti*-(EOPT)$_2$ disposition. In this section we studied the dynamical aspects of the latter interaction. Thus, the main goal is to check the stability and behavior under kinetic effects of NO-type adducts and compare them with those of the most stable NN-type adducts.

Therefore, we consider two aggregation possibilities using two models named *sg*-NO and *ag*-NO (Figure 6). The former is made of two 15-EOPT oligomer chains with all-*sg* conformation (initial dihedral angle between neighboring thiophene rings of 36.1°), whereas the latter is also made of two 15-EOPT oligomer chains but all-*ag* conformation (initial dihedral angle between neighboring thiophene rings of 120°). Both

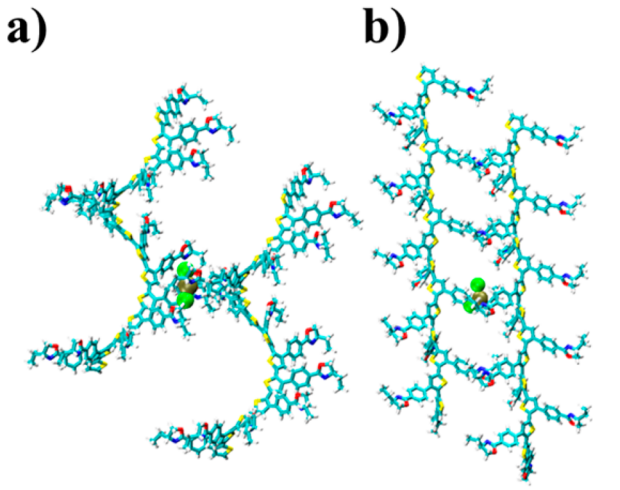

Figure 6. Schematic picture of the two initial models of [Cu(15-EOPT)$_2$]Cl$_2$ aggregates studied in this work, (a) *sg*-NO and (b) *ag*-NO.

dx.doi.org/10.1021/jp501118y | J. Phys. Chem. C 2014, 118, 9769−9779

models have the main chain axis disposed in parallel but displaced laterally at a distance of about 24.4 and 15.7 Å, respectively, allowing at least one contact site between two EOPT monomer units with one $CuCl_2$ molecule as the cross-linking element between both chains. Figure 7 shows details of contact site between the two 15-EOPT chains of a *sg*-NO model and highlights the quantum zone of the QM/MM MD simulation, which involves a total of 53 atoms.

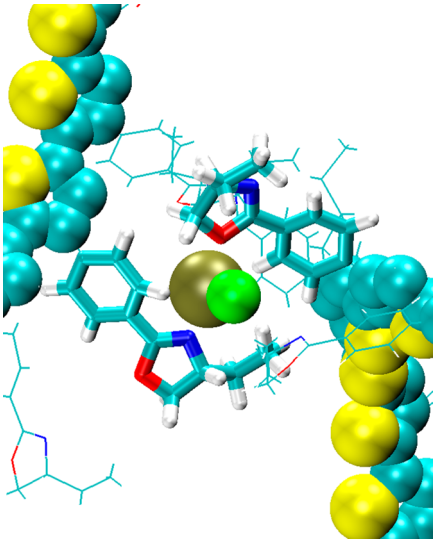

Figure 7. Model of a selected snapshot from a trajectory of *sg*-NO in explicit chloroform obtained from hybrid QM/MM MD simulation. The quantum zone is highlighted on the center which is made of two benzene and two oxazoline rings plus $CuCl_2$. The thiophene backbone is also shown, whereas chloroform molecules are deleted to obtain a clear picture.

Table 4 lists the time-averaged geometries of both *sg*-NO and *ag*-NO models during the last 6 ps of the hybrid QM/MM MD simulations in explicit chloroform. At the early stages of the simulation both models started from a similar geometry, the copper ion being situated close the neighboring oxazoline moieties. However, during simulation the two models showed a different behavior. Thus, the *sg*-NO was able to keep the cross-linked coordination during the polythiophene-backbone relaxation, whereas the *ag*-NO model was evolved toward a stable geometry with only one EOPT ligand.

The averaged *sg*-NO model approaches to the previously characterized NO′ adduct of $[Cu(EDOT)_2]Cl_2$ in chloroform (Table 3). The Cu−X and Cu−Cl bond lengths are very similar. Regarding the Cl−Cu−Cl angle, it is slightly lower for the *sg*-NO model than the NO′ adduct, which has been attributed to steric interactions and micro-oscillations provoked by explicit solvent interactions. Similarly, the dihedral angle θ is slightly larger for the *sg*-NO model (θ = 152.9°) than for the NO′ adduct (θ = 130.4°). In addition, standard deviation of the θ dihedral angle is high enough to indicate a strong oscillation around the *anti*-$(EDOT)_2$ disposition, probably due to an appreciable stress with the main chain relaxation, which leads to a more extended conformation than expected. Also, the averaged values of ξ and ω dihedral angles are slightly away from expected values of 25 to 30°, as is evidenced in Table 3, which indicates an increase of the system stress.

Moreover, the *ag*-NO model did not show any stable adduct along the simulation. In fact, the averaged geometries lead to a single EOPT ligand with a short Cu−N distance and a large Cu−O distance. The latter allows disposing the chloride ions within a plane with the copper between the two EOPT units, which is almost perpendicular to both oxazoline rings (not shown).

Variations associated with the S−C−C−S dihedral angle involving adjacent thiophene rings of the PEOPT backbone in the *ag*-NO model reveal additional stress in the NO-type adduct formation. Indeed, the dihedral angle θ between both EOPT ligands evolved from its initial value of −150° to −82°, which corresponds to the value averged during the last 2 ps of the QM/MM MD trajectory. This θ dihedral angle makes difficult a stable *anti*-$(EDOT)_2$ disposition such as that found in the previous section (Table 3). The dihedral angle ξ is related with the degree of interaction between copper metal and the EOPT ligand, and therefore, the ξ decreases with the strength of the Cu−X interaction, which is consistent with a higher resemblance with the free EOPT monomeric units. The values of ξ averaged during the last 2 ps of QM/MM MD simulation for the N- and O-interacting oxazolines are 19.1° and 1.6°, respectively. The former value is close to the most stable NN adduct of $[Cu(EOPT)_2]^{2+}$, whereas the latter implies an almost null interaction.

Figure 8 shows the chloroform distribution around the copper ion in both *ag*-NO and *sg*-NO models. The copper ion has a clear tendency to be more solvated in the *ag*-NO model than in the *sg*-NO. The former has a wider and bigger maximum than the latter when comparing both radial distribution functions and its running coordination numbers. Thus, the metallic ion is hidden among the side chain moieties with a higher difficulty to be solvated. In fact, the first maximums are located at 6.6 and 7.1 Å, with running coordination values of 12 and 32, for the *sg*-NO and *ag*-NO models, respectively.

Chirality Switching Discussion. The chirality change induced in PEOPT aggregates by metals upon the addition of poor solvent is still not well understood. This study allows the

Table 4. Comparison of Time-Averaged Geometries from the *sg*-NO and *ag*-NO QM/MM MD Simulations Calculated at the B3LYP/6-31G LANL2DZ Level in Explicit Chloroform[c]

model	d_{Cu-X}[a]	d_{Cu-Cl}	α_{ClCuCl}	θ	ξ	ω[b]
sg-NO	2.032 ± 0.062	2.306 ± 0.058	164.5 ± 5.8	152.9 ± 16.3	10.4 ± 8.8	34.3 ± 8.2
	2.228 ± 0.129	2.311 ± 0.066			−42.2 ± 12.2	40.2 ± 8.7
ag-NO	1.968 ± 0.055	2.289 ± 0.061	111.8 ± 7.9	−85.4 ± 10.8	10.4 ± 12.2	−19.5 ± 10.3
	5.181 ± 0.333	2.216 ± 0.056			17.0 ± 8.7	83.6 ± 15.8

[a]Bond distance between copper and coordinated ligand. X refers to the atom from the EOPT ligand bonded to metal. [b]Thiophene moiety atoms are out of the quantum zone. [c]Bond angle (α_{ClCuCl}) and dihedral angles (θ, ξ, and ω; see Scheme 1) in degrees; bond distances (d_{Cu-X} and d_{Cu-Cl}) in Å; averaged during the last 6 ps of the QM/MM MD trajectory.

dx.doi.org/10.1021/jp501118y | J. Phys. Chem. C 2014, 118, 9769−9779

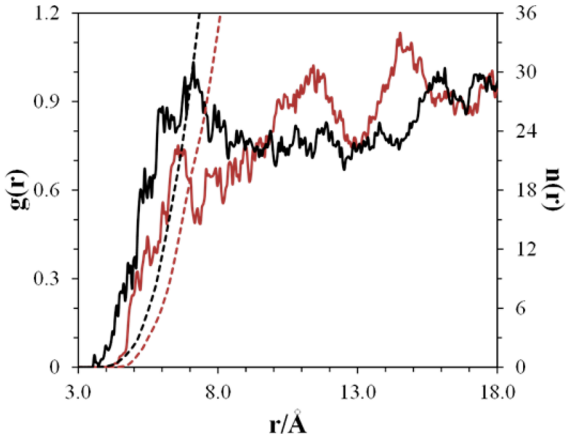

Figure 8. Copper-solvent radial distribution functions (solid lines) and running coordination (dashed lines). *sg*-NO model in brown lines and *ag*-NO model in black lines.

correlation between the structures of the most stable adducts under different situations and solvents with experimental data available. Thus, on the basis that the metal-induced aggregates of PEOPT have a mostly amorphous structure,[39] it is reasonable to expect either *syn*- or *anti*-$(EOPT)_2$ dispositions on the supramolecular aggregates. Although this makes difficult direct correlations due to the lack of a precise model for the chiral supramolecular structure, it can highlight elements clarifying the behavior observed experimentally.

The current situation, where PEOPT chiral aggregates are made by means of metallic salt addition in a nonpolar solvent such as chloroform, suggests an undissociated salt trapped by coordination with the EOPT units. This may fit in the previously studied case of the $[Cu(EOPT)_2]Cl_2$ adduct, where a predominance of *syn*-$(EOPT)_2$ dispositions involving the most stable NN-type coordination and π-stacking interactions between benzene rings of different chains was found. In a recent study devoted to PEOPT aggregation, we showed a tendency to form helical arrangements when a double chain interacts to form aggregates.[20] Thus, the *syn*-$(EOPT)_2$ disposition may favor a chiral arrangement as could be the double-stranded helical polymer complex. This coincides with the experimental work by Goto et al.,[39] which pointed to a similar supramolecular structure discarding π-stacked lamellar dispositions. Moreover, the loss of activity was experimentally observed when adding acetonitrile to the previous copper PEOPT adduct in chloroform. Goto et al.[18] suggested the possibility that the presence of acetonitrile leads to a structural change in the aggregate, which releases some Cu^{2+} that could act as an oxidizing agent on the polythiophene main chain. This partial p-doping of PEOPT would allow a change in the packing mode from chiral aggregates to a nontwisted parallel packing. This experimental evidence is consistent with the results obtained in this work for ionic $[Cu(EOPT)_2]^{2+}$ adducts in acetonitrile. In fact, the presence of Cu^{2+} as a doping ion in the adduct formation involves the change on the absolute minimum from a *syn*-$(EOPT)_2$ conformation in chloroform to *anti*-$(EOPT)_2$ conformation in acetonitrile (NN adduct, θ = 124.7°), favoring a nontwisted parallel packing as already pointed out by Goto et al.[18] Thus, both ligand orientation and the induced p-doping on the thiophene ring, which is reflected by the low dihedral angle ω observed (Table 2), may break the previous chiral structure of the double-stranded chain in chloroform stabilizing a nonchiral packing in acetonitrile with the presence of copper ions.

Another interesting point is the role that explicit molecules of acetonitrile could play. It is well-known that the copper ion tends to form stable adducts with six molecules of acetonitrile in a distorted octahedral configuration.[41,42] The $[CuEOPT]^{2+}$ adduct fills only two of the six possible ligand positions, and the rest can be occupied by acetonitrile molecules that could distort at some point the previous adduct structure of minimum energy. Thus, four acetonitrile molecules have been added to the minimum energy system (NN from Table 2) of the $[CuEOPT]^{2+}$ adduct in acetonitrile. A subsequent energy minimization led to a new structure that is shown in Figure 9,

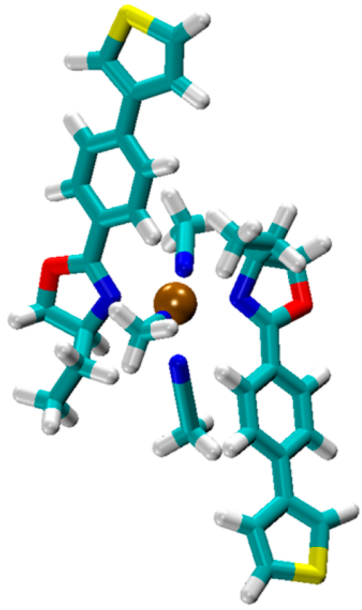

Figure 9. Minimum energy conformation obtained for $[CuEOPT_2]^{2+}$ in explicit acetonitrile.

where only three acetonitrile molecules remain attached to ligand positions. This new structure keeps the *anti*-$(EDOT)_2$ conformation, although the θ dihedral angle (θ = −149.0°) increases appreciably whereas Cu−N distances are increasing just a little bit (2.080, 2.064 Å with the oxazoline moiety and 2.124, 2.124, and 2.263 Å with acetonitrile). Interestingly, a distorted octahedral structure is obtained around the metal with one of the ligand positions blocked by ethyl and phenyl moieties of both EDOT ligands. Even though the small structural change is induced by explicit acetonitrile molecules, the *anti*-$(EDOT)_2$ conformation may still favor a nontwisted parallel packing.

Moreover, the amorphous structure of aggregates also opens the possibility to find other less populated cross-linked interactions besides the most stable NN-type, such as the less stable NO-type. The latter has been found energetically stable in neutral adducts, even though it loses stability as solvent polarity increases. However, the structural stability of NO-type adducts can break down easily depending on the amount of structural stress due to the dynamics of the main chain. Indeed, hybrid QM/MM MD simulations have shown that elongated (*all-ag*) PEOPT chains break the NO-type metal coordination, whereas the structure of the adduct made of helical chains (*all-sg*) remains stable.

dx.doi.org/10.1021/jp501118y | J. Phys. Chem. C 2014, 118, 9769−9779

CONCLUSIONS

The metal-induced aggregation of chiral PEOPT has been examined by means of studying the structural properties of $[CuEOPT]^{2+}$, $[Cu(EOPT)_2]^{2+}$, and $[Cu(EOPT)_2]Cl_2$ adducts by using ab initio quantum mechanical calculations. Different structural preferences have been found depending on the counteranion presence. Concretely, ionic adducts present a preferred angular disposition between cross-linked units of EOPT, *anti*-$(EOPT)_2$ arrangements coordinated through the most stable NN-type interaction with the copper ion being favored. On the other hand, the Cl^- anion leads to a more stable *syn*-$(EOPT)_2$ disposition through an NN-type interaction, whereas the only stable *anti*-$(EOPT)_2$ arrangement found comes through an NO-type interaction with the copper ion. The influence of the solvent and the copper ion presence points to different aggregated structures. Thus, a chiral arrangement such as a double-stranded helical polymer complex in chloroform may change to a nonchiral π-stacked packing in acetonitrile, in agreement with previous experimental evidence. Also, the possibility of weaker metal coordination on PEOPT adducts of NO-type that shows structural stability under kinetic conditions when fragments of helical chains are involved has been presented. In contrast, metal coordination breaks easily when the structure involves fragments of elongated chains of PEOPT.

AUTHOR INFORMATION

Corresponding Author

*E-mail: joan.torras@upc.edu.

Notes

The authors declare no competing financial interest.

ACKNOWLEDGMENTS

Financial support from the MINECO and FEDER (MAT2012-34498), Generalitat de Catalunya (Research group 2009 SGR925), is gratefully acknowledged. The authors are indebted to the Barcelona Supercomputer Center (BSC) for the computational resources provided. Support for the research of C.A. was received through the prize "ICREA Academia" for excellence in research funded by the Generalitat de Catalunya.

REFERENCES

(1) Cheng, P.-N.; Pham, J. D.; Nowick, J. S. The Supramolecular Chemistry of β-Sheets. *J. Am. Chem. Soc.* **2013**, *135* (15), 5477−5492.
(2) Brunsveld, L.; Folmer, B. J. B.; Meijer, E. W.; Sijbesma, R. P. Supramolecular Polymers. *Chem. Rev.* **2001**, *101* (12), 4071−4098.
(3) Bhalla, V.; Kaur, S.; Vij, V.; Kumar, M. Mercury-Modulated Supramolecular Assembly of a Hexaphenylbenzene Derivative for Selective Detection of Picric Acid. *Inorg. Chem.* **2013**, *52* (9), 4860−4865.
(4) Swiegers, G. F.; Malefetse, T. J. New Self-Assembled Structural Motifs in Coordination Chemistry. *Chem. Rev.* **2000**, *100* (9), 3483−3538.
(5) Lindoy, L. F.; Park, K.-M.; Lee, S. S. Metals, macrocycles and molecular assemblies - macrocyclic complexes in metallo-supramolecular chemistry. *Chem. Soc. Rev.* **2013**, *42* (4), 1713−1727.
(6) Roncali, J. Synthetic Principles for Bandgap Control in Linear π-Conjugated Systems. *Chem. Rev.* **1997**, *97* (1), 173−206.
(7) Skotheim, T. A.; Reynolds, J. R. *Handbook of Conducting Polymers*, 3rd ed.; CRC Press: Boca Raton, 2007.
(8) Kline, R. J.; McGehee, M. D. Morphology and Charge Transport in Conjugated Polymers. *Polym. Rev.* **2006**, *46* (1), 27−45.
(9) Cui, C. X.; Kertesz, M. Two helical conformations of polythiophene, polypyrrole, and their derivatives. *Phys. Rev. B* **1989**, *40* (14), 9661.
(10) Langeveld-Voss, B. M. W.; Janssen, R. A. J.; Meijer, E. W. On the origin of optical activity in polythiophenes. *J. Mol. Struct.* **2000**, *521* (1−3), 285−301.
(11) Li, C.; Numata, M.; Bae, A.-H.; Sakurai, K.; Shinkai, S. Self-Assembly of Supramolecular Chiral Insulated Molecular Wire. *J. Am. Chem. Soc.* **2005**, *127* (13), 4548−4549.
(12) Goto, H.; Yashima, E.; Okamoto, Y. Unusual solvent effects on chiroptical properties of an optically active regioregular polythiophene in solution. *Chirality* **2000**, *12* (5−6), 396−399.
(13) Yashima, E.; Goto, H.; Okamoto, Y. Metal-Induced Chirality Induction and Chiral Recognition of Optically Active, Regioregular Polythiophenes. *Macromolecules* **1999**, *32* (23), 7942−7945.
(14) Van den Bergh, K.; Cosemans, I.; Verbiest, T.; Koeckelberghs, G. Expression of Supramolecular Chirality in Block Copoly(thiophene)s. *Macromolecules* **2010**, *43* (8), 3794−3800.
(15) Goto, H.; Okamoto, Y.; Yashima, E. Solvent-Induced Chiroptical Changes in Supramolecular Assemblies of an Optically Active, Regioregular Polythiophene. *Macromolecules* **2002**, *35* (12), 4590−4601.
(16) Xi, X.; Jiang, L.; Sun, W.; Shen, Z. Metal-induced supramolecular chirality in optically active polymers of oxazoline-substituted N-phenylmaleimides. *Chirality* **2007**, *19* (7), 521−527.
(17) Goto, H.; Yokochi, Y.; Yashima, E. Chirality induction in metal-induced achiral polythiophene aggregates assisted by optically active amines and polythiophene. *Chem. Commun.* **2012**, *48* (27), 3291−3293.
(18) Goto, H.; Yashima, E. Electron-Induced Switching of the Supramolecular Chirality of Optically Active Polythiophene Aggregates. *J. Am. Chem. Soc.* **2002**, *124* (27), 7943−7949.
(19) Bertran, O.; Torras, J.; Alemán, C. Modeling the Structural and Electronic Properties of an Optically Active Regioregular Polythiophene. *J. Phys. Chem. C* **2010**, *114* (25), 11074−11080.
(20) Torras, J.; Sanchez-Navas, C.; Bertran, O.; Aleman, C. On the modeling of aggregates of an optically active regioregular polythiophene. *Phys. Chem. Chem. Phys.* **2012**, *14* (6), 1881−1891.
(21) Frisch, M. J.; Trucks, G. W.; Schlegel, H. B.; Scuseria, G. E.; Robb, M. A.; Cheeseman, J. R.; Scalmani, G.; Barone, V.; Mennucci, B.; Petersson, G. A., et al., *Gaussian 09*, Revision A.1; Gaussian, Inc.: Wallingford CT, 2009.
(22) Becke, A. D. A new mixing of Hartree–Fock and local density-functional theories. *J. Chem. Phys.* **1993**, *98* (2), 1372−1377.
(23) Lee, C.; Yang, W.; Parr, R. G. Development of the Colle-Salvetti correlation-energy formula into a functional of the electron density. *Phys. Rev. B* **1988**, *37* (2), 785.
(24) McLean, A. D.; Chandler, G. S. Contracted Gaussian basis sets for molecular calculations. I. Second row atoms, Z=11−18. *J. Chem. Phys.* **1980**, *72* (10), 5639−5648.
(25) Hay, P. J.; Wadt, W. R. Ab initio effective core potentials for molecular calculations. Potentials for K to Au including the outermost core orbitals. *J. Chem. Phys.* **1985**, *82* (1), 299−310.
(26) Yang, Y.; Weaver, M. N.; Merz, K. M. Assessment of the "6-31+G** + LANL2DZ" Mixed Basis Set Coupled with Density Functional Theory Methods and the Effective Core Potential: Prediction of Heats of Formation and Ionization Potentials for First-Row-Transition-Metal Complexes. *J. Phys. Chem. A* **2009**, *113* (36), 9843−9851.
(27) Boys, S. F.; Bernardi, F. The calculation of small molecular interactions by the differences of separate total energies. Some procedures with reduced errors. *Mol. Phys.* **1970**, *19* (4), 553−566.
(28) Miertus, S.; Scrocco, E.; Tomasi, J. Electrostatic interaction of a solute with a continuum. A direct utilizaion of AB initio molecular potentials for the prevision of solvent effects. *Chem. Phys.* **1981**, *55* (1), 117−129.
(29) Miertus, S.; Tomasi, J. Approximate evaluations of the electrostatic free energy and internal energy changes in solution processes. *Chem. Phys.* **1982**, *65* (2), 239−245.

(30) Cieplak, P.; Caldwell, J.; Kollman, P. Molecular mechanical models for organic and biological systems going beyond the atom centered two body additive approximation: aqueous solution free energies of methanol and N-methyl acetamide, nucleic acid base, and amide hydrogen bonding and chloroform/water partition coefficients of the nucleic acid bases. *J. Comput. Chem.* **2001**, *22* (10), 1048−1057.
(31) Wang, J.; Wolf, R. M.; Caldwell, J. W.; Kollman, P. A.; Case, D. A. Development and testing of a general amber force field. *J. Comput. Chem.* **2004**, *25* (9), 1157−1174.
(32) Preat, J.; Rodríguez-Ropero, F.; Torras, J.; Bertran, O.; Zanuy, D.; Alemán, C. Parameterization of the torsional potential for calix[4]arene-substituted poly(thiophene)s. *J. Comput. Chem.* **2010**, *31* (8), 1741−1751.
(33) Case, D. A.; Darden, T. A.; T.E. Cheatham, I.; Simmerling, C. L.; Wang, J.; Duke, R. E.; Luo, R.; Walker, R. C.; Zhang, W.; Merz, K. M., et al., *AMBER 12*; University of California: San Francisco, 2012.
(34) Berendsen, H. J. C.; Postma, J. P. M.; Gunsteren, W. F. v.; DiNola, A.; Haak, J. R. Molecular dynamics with coupling to an external bath. *J. Chem. Phys.* **1984**, *81* (8), 3684−3690.
(35) Torras, J.; Deumens, E.; Trickey, S. B. Software Integration in Multi-scale Simulations: the PUPIL System. *J. Comput. Aided Mater. Des.* **2006**, *13* (1−3), 201−212.
(36) Torras, J.; Seabra, G. d. M.; Deumens, E.; Trickey, S. B.; Roitberg, A. E. A versatile AMBER-Gaussian QM/MM interface through PUPIL. *J. Comput. Chem.* **2008**, *29* (10), 1564−1573.
(37) Bylaska, E. J.; Jong, W. A. d.; Govind, N.; Kowalski, K.; Straatsma, T. P.; Valiev, M.; Wang, D.; Apra, E.; Windus, T. L.; Hammond, J., et al. *NWChem, A Computational Chemistry Package for Parallel Computers*, 5.1; Pacific Northwest National Laboratory: Richland, Washington 99352−0999, USA, 2007.
(38) Warren, J. G.; Revilla-López, G.; Alemán, C.; Jiménez, A. I.; Cativiela, C.; Torras, J. Conformational Preferences of Proline Analogues with a Fused Benzene Ring. *J. Phys. Chem. B* **2010**, *114* (36), 11761−11770.
(39) Goto, H.; Okamoto, Y.; Yashima, E. Metal-Induced Supramolecular Chirality in an Optically Active Polythiophene Aggregate. *Chem.−Eur. J.* **2002**, *8* (17), 4027−4036.
(40) Cioslowski, J. A new population analysis based on atomic polar tensors. *J. Am. Chem. Soc.* **1989**, *111* (22), 8333−8336.
(41) Inada, Y.; Nakano, Y.; Inamo, M.; Nomura, M.; Funahashi, S. Structural Characterization and Formation Mechanism of Sitting-Atop (SAT) Complexes of 5,10,15,20-Tetraphenylporphyrin with Divalent Metal Ions. Structure of the Cu(II)−SAT Complex As Determined by Fluorescent Extended X-ray Absorption Fine Structure. *Inorg. Chem.* **2000**, *39* (21), 4793−4801.
(42) Torras, J.; Alemán, C. Determination of New Cu+, Cu2+, and Zn2+ Lennard-Jones Ion Parameters in Acetonitrile. *J. Phys. Chem. B* **2013**, *117* (36), 10513−10522.